HHS Public Access

Author manuscript

Procedia Manuf. Author manuscript; available in PMC 2021 June 28.

Published in final edited form as:

Procedia Manuf. 2020 ; 48: 332–337. doi:10.1016/j.promfg.2020.05.055.

Fabrication and Characterization of In Situ Zn-TiB_2 Nanocomposite

Zeyi Guan[a], **Gongcheng Yao**[b], **Yuxin Zeng**[a], **Xiaochun Li**[a,b,*]

[a]Department of Mechanical & Aerospace Engineering, Samueli School of Engineering, University of California, Los Angeles, 420 Westwood Pl, Los Angeles, 90005, CA, USA

[b]Department of Materials Science & Engineering, Samueli School of Engineering, University of California, Los Angeles, 420 Westwood Pl, Los Angeles, 90005, CA, USA

Abstract

Zinc (Zn) matrix composite has been newly discovered categories of biodegradable materials. With a combination of chemical stability, thermal stability and biocompatibility, ceramic nanoparticles outperformed intermetallics of zinc alloys with inherent advantages of retaining a proper corrosion rate and an exceptional ductility. Compared with Zn alloys, Zn matrix nanocomposites showed an unprecedented strengthening without sacrifices of corrosion rate, which were introduced by intermetallics. In this work, in situ titanium diboride (TiB_2) reinforced Zn nanocomposite was prepared via a few cost-effective and economical methods: flux-assisted synthesis (FAS), ultrasound-assisted nanoparticle homogenization and hot rolling. 3 vol.% of TiB_2 nanoparticles were synthesized with an average size of 454nm, followed by molten salt assisted ultrasound homogenization and hot rolling. Hot-rolled (HR) Zn-TiB_2 performed high strength and high ductility, mostly due to precipitation strengthening (Orowan strengthening). Yield stress (YS) and ultimate tensile stress (UTS) increased by 90% and 45%, respectively, while the elongation to failure retained 23%. The mechanical performance of Zn-TiB_2 made it promise to serve as an innovative biodegradable material for load-bearing applications.

Keywords

zinc matrix nanocomposite; TiB_2 in situ synthesis; biodegradable metal

1. Introduction

Zn has been studied broadly as a novel functional biodegradable material, especially for coronary vascular stent and bone implants [1], because of the excellent compatibility and tolerable corrosion rate [2, 3]. As an innovative biodegradable metal, zinc could be absorbed entirely or dissolved inside the human body, instead of leaving risks of chronic inflammation that happened for permanent metal implants, such as stainless steel [4]. Especially for

*Corresponding author. Tel.: +1(310)-825-2383; xcli@seas.ucla.edu.

Peer-review under responsibility of the scientific committee of the NAMRI/SME.

implants in orthopaedic surgery, permanent implants can hardly be applied because the rapid growth of tissue structure could outgrow the traditional metal implants, causing malfunction of the implants and other complications. Different than the maturely developed biodegradable and biocompatible metals, magnesium, Zn stands out because of its excellent biocompatibility and tolerable corrosion rate, which is theoretically suitable for bioresorbable cardiovascular stents [5]. One of the unmet properties is mechanical strength, where pure zinc obtains a low yield YS and UTS, and thus it cannot be utilized for load-bearing applications. The alloying method provides efficient strengthening, but the introduction of the intermetallic phases usually results in an increased corrosion rate [6] and deterioration in cell viability [1]. Moreover, the additional elements, such as aluminum, could cause potential human body inflammation responses [7]. Alloys like Zn-Mg and Zn-Li are options that achieved a combination of high strength, high elongation to failure, degradability, and biocompatibility after severe deformation. Still, their weakness in thermal stability resulted in rapid natural aging, where they lost ductility within a few days [8, 9].

An alternative strengthening method is by introducing dispersed nanoparticles as reinforcements, e.g., tungsten carbide (WC) nanoparticles [10], silicon carbide (SiC) nanoparticles [11], alumina (Al_2O_3) [12], hydroxyapatite (HA) [13] for zinc matrix nanocomposite. Nanoparticles provide precipitation strengthening by impeding the dislocation [14], grain refinement [15] and increasing the dislocation density [16]. For example, previous work has shown that hot-rolled Zn-4.4 vol.%WC achieved more than 50% strength enhancement while retaining more than 70% in elongation to failure [10]. More importantly, due to the chemical and thermal stability of the ceramic nanoparticles [17], the corrosion rate of nanocomposite could theoretically be maintained at the same level of zinc and body temperature natural annealing/natural aging effect could be inhibited by nanoparticles pinning effect [18–20]. Although nano-reinforcement has been proven to be an efficient strengthening strategy, nearly most of the fabrication methods of Zn matrix nanocomposite are high energy planetary ball milling. The relatively high cost and inefficiency of material processing make this process difficult to be applied to industrial production. An urgent need for a highly scalable and applicable method is required for the fabrication of the Zn matrix nanocomposite with a combination of enhanced strengthen and ductility.

In this work, TiB_2 was incorporated into the pure Zn matrix and homogeneously dispersed through the in-situ synthesis method, known as flux assisted synthesis (FAS), with the addition of salt-assisted ultrasound processing and hot rolling [21, 22]. The microstructure characterization of hot-rolled Zn-3vol.% TiB_2 nanocomposite has been performed for nanoparticle size and distribution. Furthermore, the mechanical characterization was carried out to test the strength and ductility.

2. Method

2.1. Zn-TiB_2 nanocomposite manufacturing

FAS were used for TiB_2 particle synthesis and incorporation into the Zn matrix. High purity Zn (99.995%, ingot, Rotometal) and aluminium (Al) (99.999%, ingot, Alfa aesar) were used as the raw materials. Zn and Al (5 wt%) were melted at a temperature of 700°C. Mixed salt

of potassium tetrafluoroborate (KBF_4), potassium hexafluorotitanate (K_2TiF_6) with a design of 3 vol.% TiB_2 was added into the ZnAl melt, with an atomic ratio of 2B/Ti, shown in Fig. 1(a). The reaction of salt in the metal melt to synthesize TiB_2 nanoparticles according to reactions:

$$3K_2TiF_6 + 13Al = 3Al_0Ti + 3KAlF_4 + K_3AlF_6 \quad (1)$$

$$2KBF_4 + 3Al = AlB_2 + 2KAlF_4 \quad (2)$$

$$AlB_2 + Al_3Ti = TiB_2 + 4Al \quad (3)$$

The molten salts were manually stirred for 10 minutes and salt slug were removed. New chloride salt (1:1:1 atomic ratio NaCl/KCl/ZnCl) was added, and ultrasound was applied by an ultrasonic liquid processor (Misonix S-4000) installed with a Niobium probe for 10 minutes to remove the salt trapped in the metal melt at 500°C, to dispersed nanoparticles and to react with the Al residue in the metal melt, shown in Fig. 1(b). Zn-TiB_2 was then cast in a steel mold, shown in Fig. 1(c). The nanocomposite samples went through hot cross-rolling (75% thickness reduction) at 250°C, shown in Fig. 1(d).

2.2. Characterization methods

The high purity Zn and Zn-3vol%TiB_2 nanocomposite samples, both in hot rolling conditions, were prepared by mechanical grinding, alumina nanoparticle polishing and ion milling polishing for microstructure characterization using a scanning electron microscopy (ZEISS Supra 40VP SEM). The dispersion and size distribution of in situ TiB_2 nanoparticles was also investigated by SEM and energy-dispersive x-ray spectroscopy (EDS) analysis, with image processing through Image Pro. Microhardness test was performed covering the entire samples by LM 800AT microhardness tester using a load of 200gf with a 10s dwell time. The tensile testing specimens were fabricated by electrical discharge machining (EDM). The gage length and width of the tensile specimens were 10 mm and 4 mm, respectively (ASTM E8/E8M standard sub-size). Tensile tests were carried out using Instron ElectroPlus 1000 at a strain rate of 2 mm/min. 0.2% proof stress was used as yield strength.

3. Result

3.1. Microstructure

Typical SEM images of TiB_2 nanoparticles were synthesized and dispersed within the zinc matrix, owing to the assistance of the ultrasound processing and plastic deformation (e.g. hot rolling), shown in Fig. 2(a). The aluminium residue was not observed through EDS map scanning. Darker phases represented the TiB_2 nanoparticles, and the brighter phases were the zinc matrix. Nanoparticle clusters of tens of micrometers were observed, which indicated non-homogeneous dispersion in local areas. However, nanoparticles were homogeneously dispersed within these pseudo clusters, without agglomeration and sintering, shown in magnified Fig. 2(b). The corresponding Fig. 2(e) and 2(f) were the EDS scanning intensity

of Zn and titanium(Ti), in Fig. 2(b). There were also areas of coarsely dispersed TiB_2 nanoparticles, shown in Fig. 2(c).

EDS point scanning was applied to distinguish and confirm that TiB_2 nanoparticles were synthesized in the method abovementioned, shown in Fig. 3. Point 1 indicated the darker phase area represented Ti elements, where Point 2 indicated the brighter phases represented the Zn matrix.

3.2. Nanoparticle size analysis

A typical SEM image was captured for image processing of the nanoparticle size characterization (over than 200 TiB_2 nanoparticles), shown in Fig. 4a. The corresponding histogram of TiB_2 nanoparticle size distribution was shown in Fig. 4b. The size of TiB_2 nanoparticles primarily falls in the range of 300–600 nm with an average value of 454±192 nm.

3.3. Microhardness characterization

Vickers microhardness of HR Zn-3TiB_2 was compared with HR Zn, shown in Fig. 5. This data indicated that 3 vol.% of TiB_2 nanoparticles have remarkably enhanced the hardness over 85%, from 34.4HV to 63.9HV. Compared with Al-TiB_2, another TiB_2 reinforced metal matrix nanocomposite system, in which 5 wt.% nanoparticles have only provided 10–20% hardness improvement[23], Zn-TiB_2 system has shown a significant efficiency on the improvement of hardness, indicating a fairly effective strengthening mechanism.

3.4. Tensile test

Mechanical behaviors of HR Zn-3vol.%TiB_2 and HR Zn have been further characterized by tensile testing, and the representative engineering stress-strain curves were shown in Fig. 6a. UT, YS, and elongation to failure have been modified from 98.9MPa to 143.8MPa, 36.6MPa to 70.2MPa, 71.9% to 22.8%, respectively. The results of the tensile properties are shown in Fig 6b. Fracture surface SEM images of HR zinc and HR Zn-3TiB_2 were shown in Fig. 6c and Fig 6d, respectively. Arrows have indicated the dimples, which are the typical ductile fracture.

4. Discussions

FAS has been used to produce TiB_2 nanoparticles in the Zn alloy matrix for strengthening, due to the excellent compatibility between the lattice distances of the hexagonal crystal structures of TiB_2 and η-Zn phases [22]. The dispersion was attributed to the excellent wettability between molten Zn and TiB2 nanoparticles [24]. Following the similar manufacturing method, this work has performed with extra molten salt-assisted ultrasound processing to get rid of the aluminium and disperse the nanoparticle. Further hot rolling was applied for the grain refinement due to the dynamic recrystallization and the nanoparticle dispersion homogenization [25]. With 75% thickness reduction, Zn-3vol.%TiB_2 nanocomposites maintained a high elongation to failure, further indicating the relatively good dispersion of nanoparticle with no particle agglomeration. Furthermore, the results showed a reasonable and comparable UTS where Zn-4.4vol.%WC nanocomposites shown

160 MPa in UTS. The combination of high strength and high ductility outperforms many zinc alloys and satisfies the standard requirement for biodegradable vascular stent applications [3].

Compared with Zn matrix nanocomposite fabricated by powder metallurgy, which could also achieve relatively good dispersion, this work has stood out with large volume fabrication, and the standard size tensile bars were fabricated in the process. Tensile properties tested in this work are more meaningful than the microhardness test and compression test when being utilized for biomedical applications. Such data have never been acquired for composite material produced in other research.

The strength enhancement is due to multiple mechanisms and effects, including the precipitation-induced Orowan strengthening (Eq. 4), the grain boundary-induced Hall-Petch effect (Eq. 5), and load-bearing (Eq. 6).

$$\Delta\sigma_{Orowan} = \frac{\varphi G b}{d_p}\left(\frac{6V_p}{\pi}\right)^{\frac{1}{3}} = \frac{2\times 35GPa\times 0.266nm}{454nm}\times\left(\frac{6\times 0.03}{\pi}\right)^{1/3} = 15.7MPa \quad (4)$$

where G_m, b, V_p, and d_p are the shear modulus of the matrix, the Burgers vector, the volume fraction and the size of the nanoparticles, respectively. φ is constant.

$$\Delta\sigma_{HP} = k\cdot d^{-\frac{1}{2}} = 6.8MPa\sqrt{mm}\times 0.05^{-\frac{1}{2}} = 30.4MP \quad (5)$$

where d is the grain size and k is a constant. Although this work has not comprehensively tested the grain size of the nanocomposite samples, 50 um grain size was estimated conservatively through other Zn nanocomposite works [10].

$$\Delta\sigma_{load} = 1.5V_p\sigma_i \quad (6)$$

where σ_i is the interfacial bonding strength. TiB_2 typically has a high interfacial bonding strength with metals, especially aluminum, due to the excellent wettability [26]. However, such exact strength enhancement is unable to be calculated here.

Further optimization of nanoparticle concentration will be required for a better combination for the specific applications as biomaterials. Although TiB_2 is commonly concerned as highly stable nanoparticles with the resistance of high temperature, corrosive and reactive environment, its biocompatibility will need to be tested on whether human cells would have negative responses when in contact. Another essential future work would be the in vivo characterization for Zn-TiB_2 nanocomposite on verifying whether nanoparticles would be successfully circulated and get out of the animal in time.

5. Conclusions

This study performed in situ Zn-3TiB_2 metal matrix nanocomposite fabrication through FAS, ultrasound processing and hot rolling. TiB_2 nanoparticles were synthesized with an average size of 454nm and homogeneously dispersed within the zinc matrix. With 3 vol.% TiB_2 nanoparticles, the mechanical strength of zinc has been significantly improved by, 85%

for microhardness, 90% for YS and 45% for UTS. The ductility of zinc retained retain in 22.8%, which is high enough for applications such as a biodegradable vascular stent. Generally, Zn-TiB_2 nanocomposite has provided both high strength and high ductility, offering an alternative method of strengthening for an abundance of load-bearing applications, such as biodegradable medical devices.

Acknowledgements

The research reported in this publication was supported by the National Heart, Lung, And Blood Institute of the National Institutes of Health under Award Number R01HL143465. The content is solely the responsibility of the authors and does not necessarily represent the official views of the National Institutes of Health.

References

[1]. Yang H, Jia B, Zhang Z, Qu X, Li G, Lin W, Zhu D, Dai K, Zheng Y, Alloying design of biodegradable zinc as promising bone implants for load-bearing applications, Nature Communications, 11 (2020) 1–16.

[2]. Katarivas Levy G, Goldman J, Aghion E, The prospects of zinc as a structural material for biodegradable implants—A review paper, Metals, 7 (2017) 402.

[3]. Bowen PK, Drelich J, Goldman J, Zinc exhibits ideal physiological corrosion behavior for bioabsorbable stents, Advanced materials, 25 (2013) 2577–2582. [PubMed: 23495090]

[4]. Voggenreiter G, Leiting S, Brauer H, Leiting P, Majetschak M, Bardenheuer M, Obertacke U, Immuno-inflammatory tissue reaction to stainless-steel and titanium plates used for internal fixation of long bones, Biomaterials, 24 (2003) 247–254. [PubMed: 12419625]

[5]. Ma J, Zhao N, Zhu D, Endothelial cellular responses to biodegradable metal zinc, ACS biomaterials science & engineering, 1 (2015) 1174–1182. [PubMed: 27689136]

[6]. Gong H, Wang K, Strich R, Zhou JG, In vitro biodegradation behavior, mechanical properties, and cytotoxicity of biodegradable Zn–Mg alloy, Journal of Biomedical Materials Research Part B: Applied Biomaterials, 103 (2015) 1632–1640.

[7]. De Chambrun GP, Body-Malapel M, Frey-Wagner I, Djouina M, Deknuydt F, Atrott K, Esquerre N, Altare F, Neut C, Arrieta M, Aluminum enhances inflammation and decreases mucosal healing in experimental colitis in mice, Mucosal immunology, 7 (2014) 589. [PubMed: 24129165]

[8]. Jin H, Zhao S, Guillory R, Bowen PK, Yin Z, Griebel A, Schaffer J, Earley EJ, Goldman J, Drelich JW, Novel high-strength, low-alloys Zn-Mg (< 0.1 wt% Mg) and their arterial biodegradation, Materials Science and Engineering: C, 84 (2018) 67–79.

[9]. Zhao S, McNamara CT, Bowen PK, Verhun N, Braykovich JP, Goldman J, Drelich JW, Structural characteristics and in vitro biodegradation of a novel Zn-Li alloy prepared by induction melting and hot rolling, Metallurgical and Materials Transactions A, 48 (2017) 1204–1215.

[10]. Guan Z, Pan S, Linsley C, Li X, Manufacturing and Characterization of Zn-WC as Potential Biodegradable Material, Procedia Manufacturing, 34 (2019) 247–251. [PubMed: 34007864]

[11]. Gao C, Yao M, Shuai C, Peng S, Deng Y, Nano-SiC reinforced Zn biocomposites prepared via laser melting: microstructure, mechanical properties and biodegradability, Journal of Materials Science & Technology, 35 (2019) 2608–2617.

[12]. Karimzadeh F, Enayati M, Tavoosi M, Synthesis and characterization of Zn/Al2O3 nanocomposite by mechanical alloying, Materials Science and Engineering: A, 486 (2008) 45–48.

[13]. Yang H, Qu X, Lin W, Wang C, Zhu D, Dai K, Zheng Y, In vitro and in vivo studies on zinc-hydroxyapatite composites as novel biodegradable metal matrix composite for orthopedic applications, Acta biomaterialia, 71 (2018) 200–214. [PubMed: 29530820]

[14]. Chen L-Y, Xu J-Q, Choi H, Pozuelo M, Ma X, Bhowmick S, Yang J-M, Mathaudhu S, Li X-C, Processing and properties of magnesium containing a dense uniform dispersion of nanoparticles, Nature, 528 (2015) 539. [PubMed: 26701055]

[15]. Heidarzadeh A, Pouraliakbar H, Mahdavi S, Jandaghi MR, Ceramic nanoparticles addition in pure copper plate: FSP approach, microstructure evolution and texture study using EBSD, Ceramics International, 44 (2018) 3128–3133.

[16]. Yang Y, Lan J, Li X, Study on bulk aluminum matrix nano-composite fabricated by ultrasonic dispersion of nano-sized SiC particles in molten aluminum alloy, Materials Science and Engineering: A, 380 (2004) 378–383.

[17]. Xiao P, Ge X, Wang H, Liu Z, Fisher A, Wang X, Novel molybdenum carbide–tungsten carbide composite nanowires and their electrochemical activation for efficient and stable hydrogen evolution, Advanced Functional Materials, 25 (2015) 1520–1526.

[18]. Cao C, Yao G, Jiang L, Sokoluk M, Wang X, Ciston J, Javadi A, Guan Z, De Rosa I, Xie W, Bulk ultrafine grained/nanocrystalline metals via slow cooling, Science advances, 5 (2019) eaaw2398. [PubMed: 31467973]

[19]. Lin T-C, Cao C, Sokoluk M, Jiang L, Wang X, Schoenung JM, Lavernia EJ, Li X, Aluminum with dispersed nanoparticles by laser additive manufacturing, Nature communications, 10 (2019) 1–9.

[20]. Guan Z, Linsley CS, Hwang I, Yao G, Wu BM, Li X, Novel zinc/tungsten carbide nanocomposite as bioabsorbable implant, Materials Letters, 263 (2020) 127282. [PubMed: 32647402]

[21]. Chen D, Zhao Y, Li G, Zheng M, Chen G, Mechanism and kinetic model of in-situ TiB 2/7055Al nanocomposites synthesized under high intensity ultrasonic field, Journal of Wuhan University of Technology-Mater. Sci. Ed, 26 (2011) 920–925.

[22]. Li Z, Fabrication of in situ TiB2 particulates reinforced zinc alloy matrix composite, Materials Letters, 121 (2014) 1–4.

[23]. Nagercoil KD, Tribological, tensile and hardness behavior of TiB2 reinforced aluminium metal matrix composite, Journal of the Balkan Tribological Association Vol, 20 (2014) 380–394.

[24]. Chen F, Wang T.-m., Chen Z.-n., Mao F, Han Q, Cao Z.-q., Microstructure, mechanical properties and wear behaviour of Zn-Al-Cu-TiB2 in situ composites, Transactions of Nonferrous Metals Society of China, 25 (2015) 103–111.

[25]. Liu W, Hu X, Wang X, Wu K, Zheng M, Evolution of microstructure, texture and mechanical properties of SiC/AZ31 nanocomposite during hot rolling process, Materials & Design, 93 (2016) 194–202.

[26]. Zhang L, Li B, Wu H, Wang W, Zhai S, Xu J, Niu Z, Wang Y, Microstructure and property characterization of Al-based composites reinforced with CuZrAl particles fabricated by mechanical alloying and spark plasma sintering, Advanced Powder Technology, 29 (2018) 1695–1702.

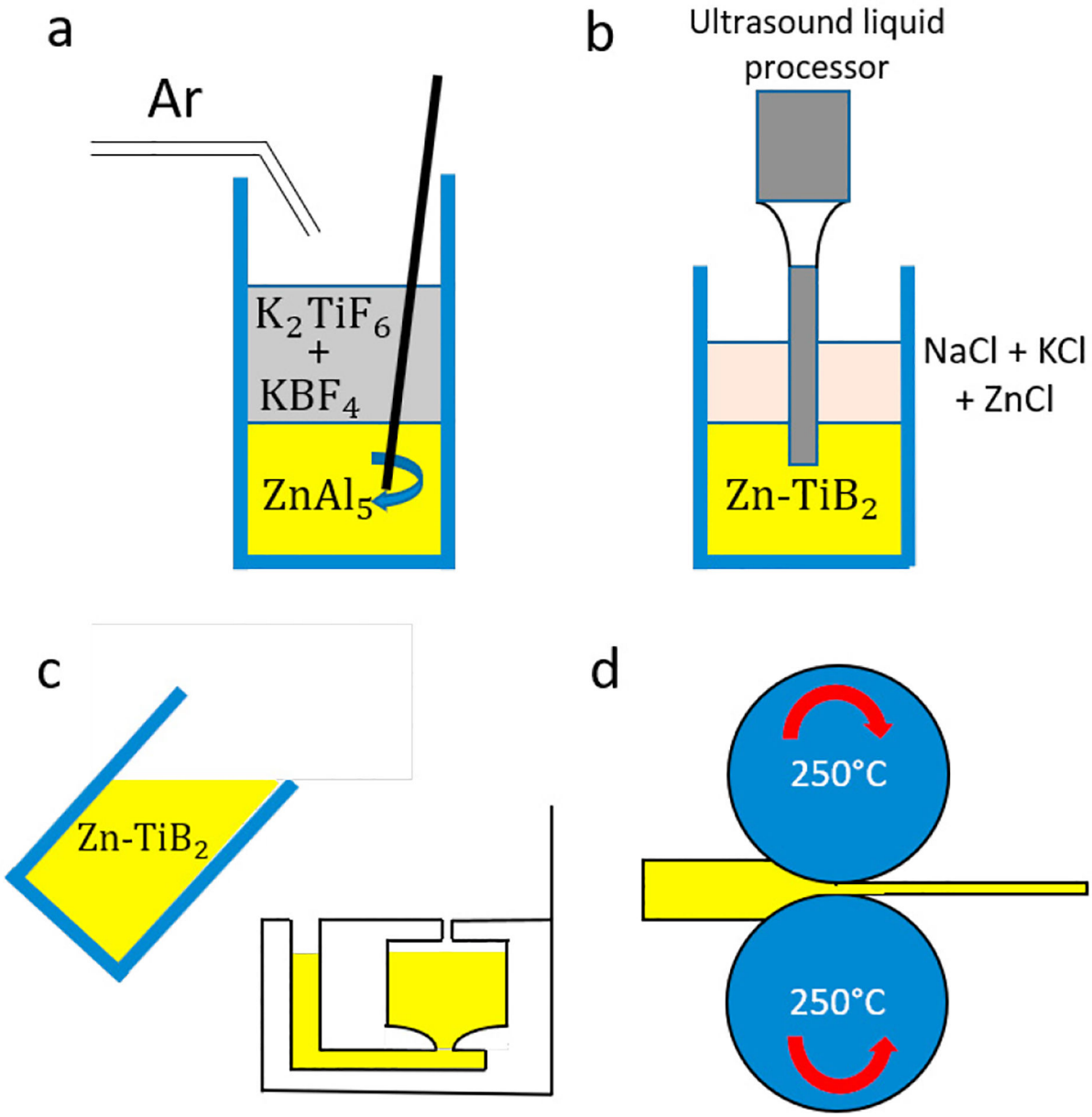

Figure 1:
Schematics of Zn-TiB_2 fabrication procedure: (a) FAS for nanoparticle synthesis and incorporation, (b) molten salt assisted ultrasound processing for homogeneous nanoparticle dispersion, (c) casting in a steel mold, (d) hot rolling.

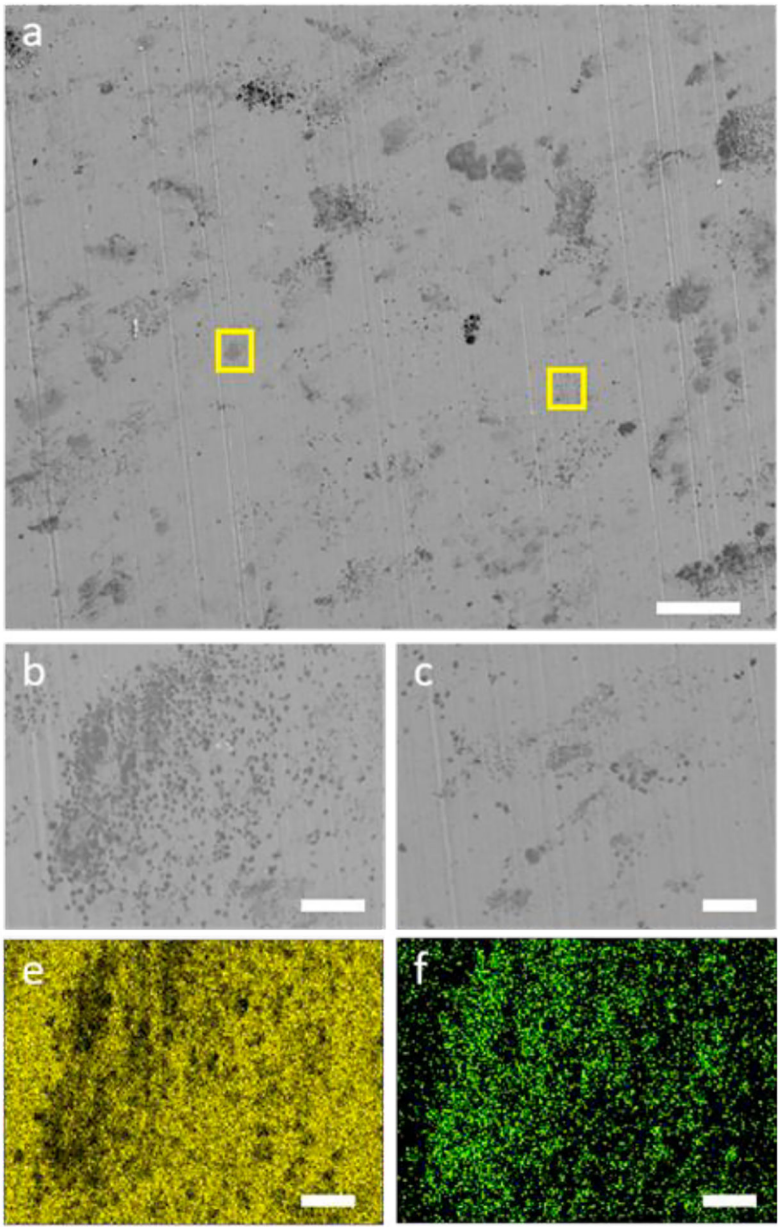

Figure 2:

(a) Typical SEM images of Zn-3TiB_2 nanocomposite. (b) and (c) show the zoom-in SEM images at the local area, indicated in (a). Micrometer size pseudo-clusters containing many nanoparticles were observed. (e) and (f) correspond to the EDX scanning element intensity of Zn and Ti, respectively, shown in the local area (b), Scale bars indicate 20 um in (a) and 5 um in (b-f).

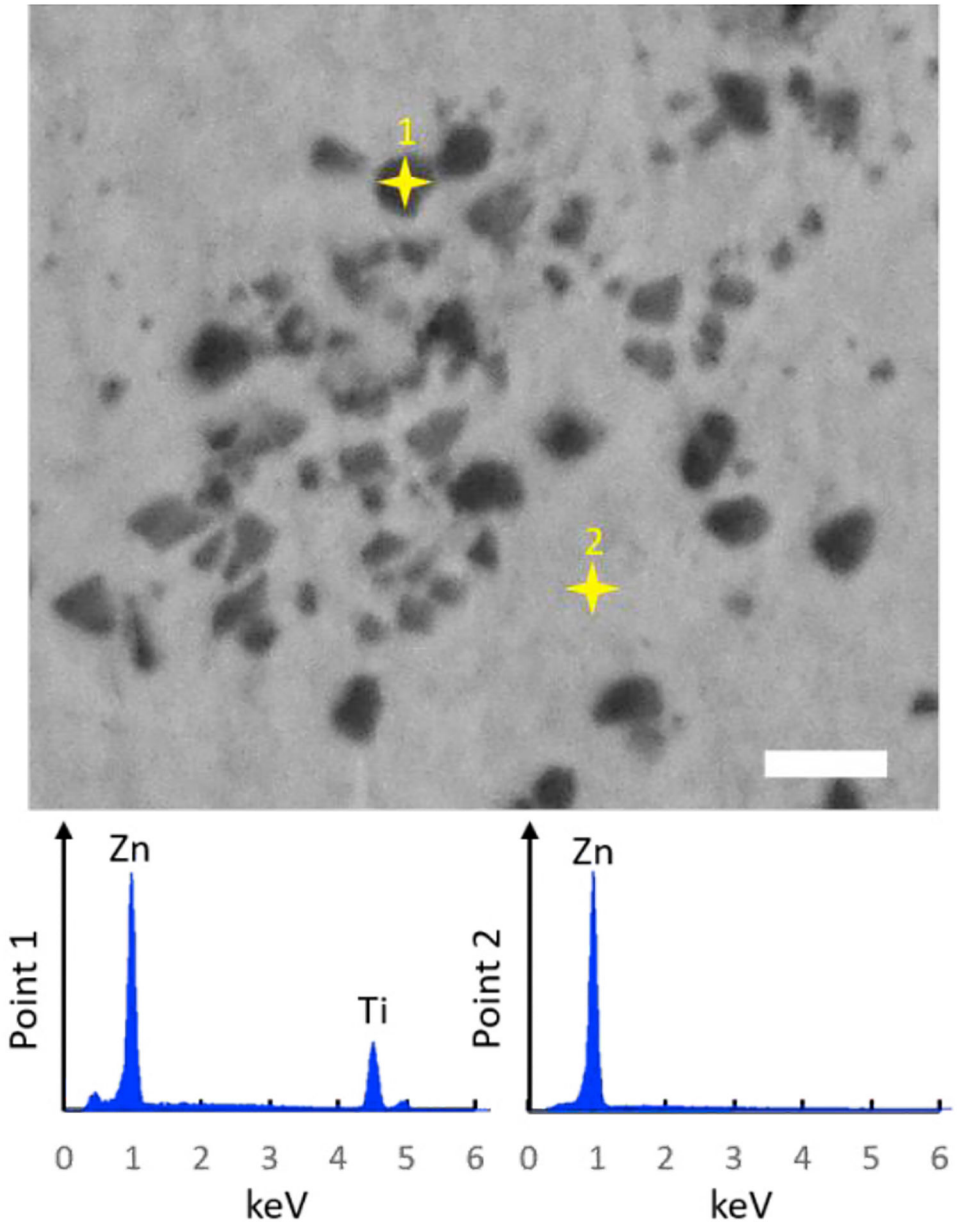

Figure 3:
EDS point scanning on Zn-3TiB_2 samples to distinguish nanoparticles and matrix elements. Scale bar represents 1 um.

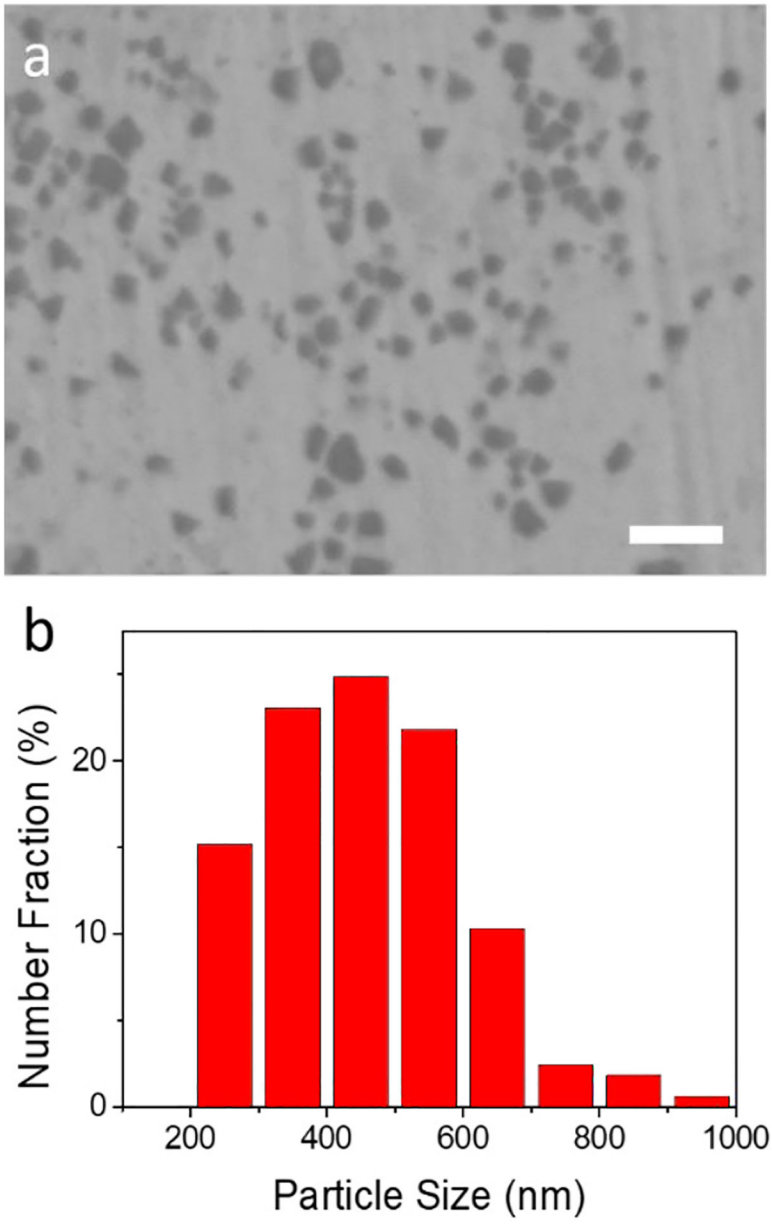

Figure 4:
(a) SEM images of Zn-3TiB_2 under high magnification. (b) histogram of nanoparticle distribution after imaging processing. Scale bars indicate 1um.

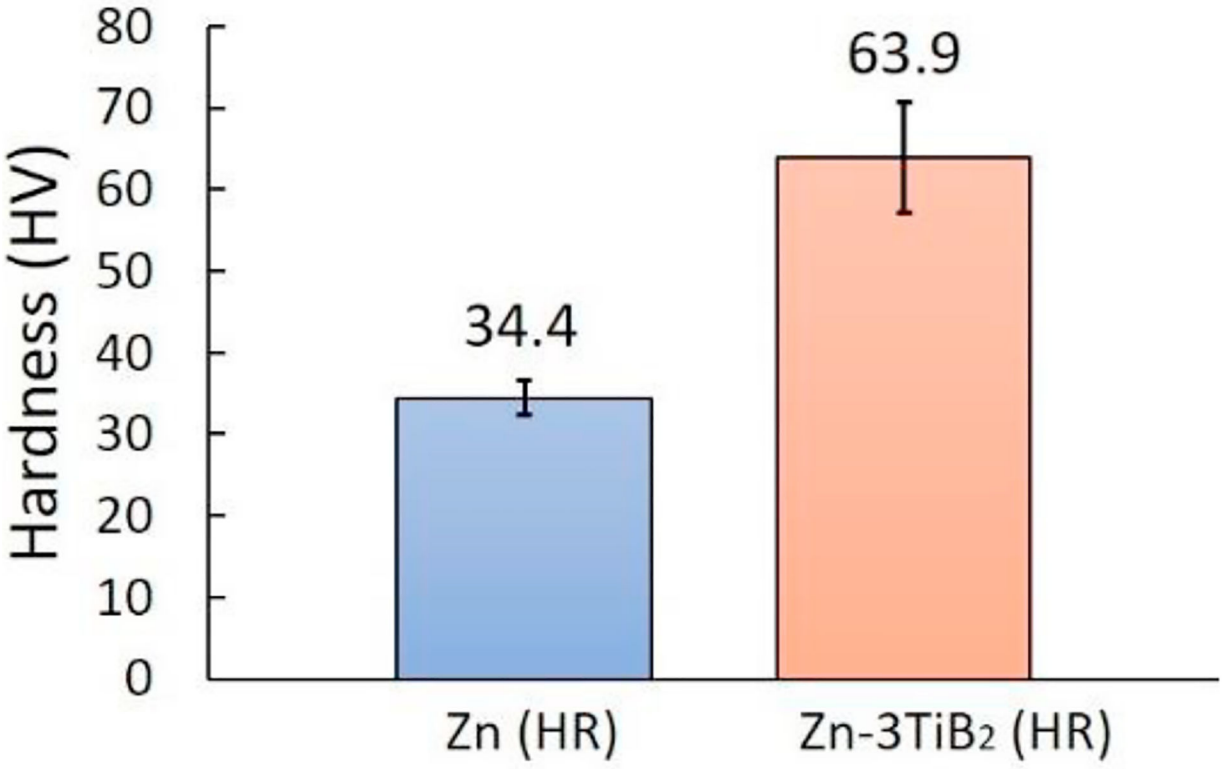

Figure 5:
Microhardness of Zn and Zn-3TiB_2 nanocomposite

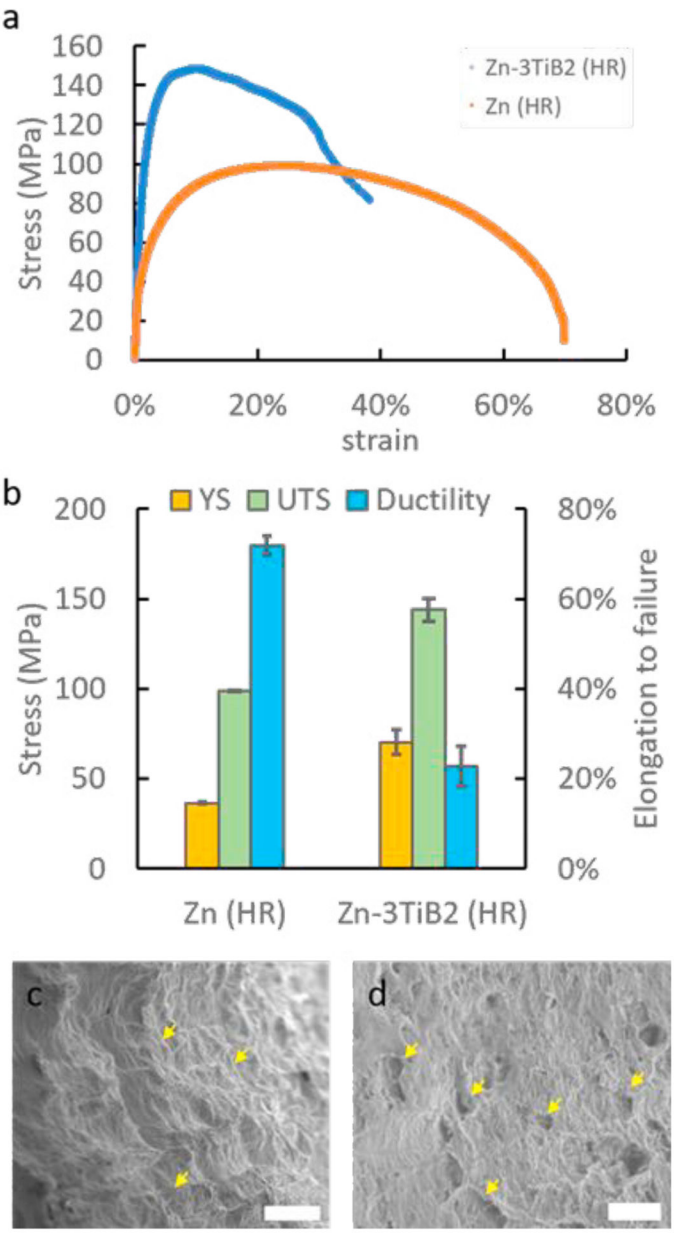

Figure 6:

(a)Stress-strain curve of Zn and Zn-TiB_2. (b) Mechanical properties by the tensile test). Fracture surfaces of the tensile test specimen for Zn(c) and Zn-3TiB_2(d). Ductile dimples are indicated by arrows. Scale bars indicate 20um.